Mixed Hydrates of Methane and Water-Soluble Hydrocarbons Modeling of Empirical Results

R. M. de Deugd, M. D. Jager, and J. de Swaan Arons
Dept. of Chemical Technology, Laboratory of Applied Thermodynamics and Phase Equilibria, Delft University of Technology, 2628 BL Delft, The Netherlands

The hydrate disappearance conditions ($H - L_w - V \rightarrow L_w - V$ transition) in the water–methane–water-soluble hydrocarbon system were measured and modeled. The hydrocarbons in the experiments are tetrahydrofuran (THF), 1,3-dioxolane and tetrahydropyran, and THF, 1,3-dioxolane and acetone in the modeling study. Experiments and calculations, which correspond qualitatively and quantitatively very well, show a large reduction in the equilibrium pressure upon addition of the hydrocarbons. The minimum pressure is about 5–6 mol % hydrocarbon relative to water, independent of temperature and applied hydrocarbon, with the composition almost equal to the ratio between the number of large cages and water molecules in structure II hydrates (5.88%). Based on this observation, the hydrates are assumed to be structure II methane–hydrocarbon mixed hydrates. The model is also used to calculate the occupancies of the hydrate cavities. No experimental data are available to compare the predicted values, but the results help understand observed phenomena better.

Introduction

Natural-gas hydrates are icelike compounds consisting of water and one or more other hydrate-forming compounds. The hydrate lattice contains certain cavities, which should at least partially be filled with the hydrate-forming compound. Without the presence of the compound filling the hydrate cavities the hydrate lattice is unstable and will therefore not exist. The hydrate formers are typically low molecular-weight compounds like methane, ethane, or carbon dioxide, but in certain cases also larger molecules such as tetrahydrofuran (THF), 1,3-dioxolane, and acetone can fit in the hydrate cavities. Three different hydrates structures (I, II, and H) are known. Each structure has its own composition of cavities of various sizes. The structure that is formed in a certain system depends strongly on the composition.

Hydrates are not only of academic interest but are also problematic to the oil and gas industry, as natural-gas hydrate formation can lead to the plugging of gas transportation lines. A potential application of hydrates may be in natural-gas storage and transportation. The high equilibrium pressures of natural-gas hydrates are a major drawback in this application.

In recent years several articles (Ng and Robinson, 1996; Mainusch et al., 1997; Saito et al., 1996; Jager et al., 1999) have been published that describe the reduction of hydrate equilibrium pressures by adding small concentrations of water-soluble organic compounds. Addition of organic compounds in smaller concentrations than 5 mol % relative to water lowers the equilibrium pressure at a given temperature significantly, while addition of higher concentrations diminishes the pressure-reducing effect.

Ng and Robinson (1996) showed this effect in the water–methane–acetone system, in which acetone is the soluble hydrate stabilizer. Research by Mainusch et al. (1997) in our laboratory confirmed the findings in the acetone system by Ng and Robinson. Saito et al. used several other organic compounds, such as THF, 1,4-dioxane, and 1,3-dioxolane (Saito et al., 1996; Saito, personal communication, 1996). Their results show similar behavior to that shown by Ng and Robinson and Mainusch et al. In our previous article (Jager et al., 1999), we reported an experimental and modeling investigation, with 1,4-dioxane as the water soluble hydrate sta-

Correspondence concerning this article should be addressed to J. de Swaan Arons.
Present address of: R. M. de Deugd, Dept. of Chemical Technology, Section Industrial Catalysis, Delft University of Technology, 2628 BL Delft, The Netherlands; M. D. Jager, Dept. of Chemical Engineering and Petroleum Refining, Center for Hydrate Research, Colorado School of Mines Golden, CO 80401.

bilizer. The present contribution is a continuation of this effort using a revised model.

The equilibrium pressure reduction effect by water–soluble compounds differs from the pressure effect of other compounds by its concentration dependency. Insoluble stabilizers like benzene, cyclohexane, cyclopentane, neopentane, and methylcyclopentane, as described by Tohidi and coworkers (Tohidi et al., 1996, 1997a,b; Danesh et al., 1993, 1994), form an extra liquid phase in the system, which reduces by one the number of degrees of freedom according to the Gibbs phase rule. This results in the absence of concentration dependence on the hydrate equilibrium pressure.

Systems containing water-soluble additives lose their concentration dependency if the solubility limit is reached, if applicable. Examples of this phenomenon are the water–methane–tetrahydropyran system and the water–methane–1,3-dioxolane–sodium chloride system. The solubility of tetrahydropyran in water is about 1.5 mol % (Bennet and Philips, 1928). Systems exceeding this concentration form an additional liquid phase and lose the concentration dependency of the hydrate equilibrium conditions. The same phenomenon is observed in the water–methane–1,3-dioxolane–sodium chloride system. 1,3-Dioxolane is completely miscible with water, but the solubility is reduced dramatically by the addition of sodium chloride. This again results in an extra liquid phase and loss of concentration dependency (De Deugd et al., unpublished results, 1998).

The earlier hydrate modeling effort has to be modified if these mixed hydrate systems are to be modeled. None of these models can predict hydrate formation by water-soluble hydrate formers, since they assume that the concentration of hydrate formers in the water phase is very low. In such cases, the activity of water is not influenced dramatically and the activity coefficient can be approximated as being one. The described concentration-dependent pressure reduction effect requires another approach, because the aqueous liquid phase contains a large number of hydrate formers. The activity coefficients of the components in the aqueous liquid phase deviate from one and must be described by means of an activity coefficient model.

Until now, two studies have been published on modeling mixed hydrate systems containing water-soluble organic hydrate formers. Mainusch et al. (1997) describe hydrate formation using a hydrate inhibition model. Jager et al. (1999) use a model based on the statistical thermodynamical approach originally introduced by Van der Waals and Platteeuw (1959). As mentioned earlier, the present contribution is a continuation and extension of the work done by Jager et al. (1999).

The discussed systems can have practical importance for several potential applications in which hydrates are used. Examples are the storage and transportation of gases like natural gas. The addition of the organic compounds lowers the hydrate equilibrium pressure at a given temperature, or stated differently, raises the hydrate equilibrium temperature at a given pressure. This effect can be advantageous in technologies that make use of single hydrates. Economic, safety, and environmental aspects are also important.

The presence study reports experimental and calculation results of hydrate formation in systems containing water, methane, and water-soluble organic compounds. The organic compounds in this report are acetone, 1,3-dioxolane, tetrahydrofuran (THF), and tetrahydropyran (THP). This article contains both experimental and modeling results of systems, with 1,3-dioxolane and THF as the organic compound. In the case of the system containing acetone, we only present modeling results using the experimental data by Mainusch et al. (1997) and Ng and Robinson (1996). Due to the lack of data on the activity in the liquid phase, we had to limit our consideration of the THP system to experimental results.

The experimental results report data on the $H - L_w - V \rightarrow L_w - V$ transition in systems with water–methane and the water-soluble organic compound just mentioned.

The model is based on the theory proposed by Van der Waals and Platteeuw (1959) and on the modifications Parrish and Prausnitz (1972) made to describe the hydrate phase. The aqueous liquid phase is modeled using an equation proposed by Holder et al. (1980). The activity coefficient models are the Van Laar equations in the case of the water–methane–acetone and water–methane–THF systems and the Wilson equations for the water–methane–1,3-dioxolane system. The coefficients in the equations are obtained from the activity coefficient at infinite dilution for the Van Laar model and from vapor–liquid equilibria in the case of the Wilson model.

Experimental Studies

All experiments have been carried out in a high-pressure Cailletet apparatus. De Loos et al. (1993) have discussed the design and principle of this equipment before. The details of the experimental procedure also have been described extensively by Coorens et al. (1988). The accuracy of pressure measurement is 0.001 MPa, and the temperature has been measured with an accuracy of 0.01 K.

This article describes experiments determining the $H - L_w - V \rightarrow L_w - V$ hydrate disappearance conditions in systems containing water, methane, and a water-soluble organic compound. The applied organic compounds in this study are 1,3-dioxolane, tetrahydrofuran (THF), and tetrahydropyran (THP). The experiments with 1,3-dioxolane have been carried out with seven different compositions (1, 2.5, 4.2, 5, 7.1, 10 and 20 mol % relative to water). In the case of the experiments with THF, three different compositions (1, 5, 10 mol % relative to water) have been applied. The water–methane–THP system has only been investigated at one composition (1 mol % relative to water).

In the experiments the $H - L_w - V \rightarrow L_w - V$ transition temperatures were determined at different constant pressures for each composition. The applied pressures were 2, 3.5, 5, 6.5, 8, 9.5, 11, 12.5, and 14 MPa. At a fixed pressure, the temperature is raised until the last tiny hydrate crystal disappears from the mixture of hydrate, aqueous liquid, and vapor.

Table 1 summarizes the suppliers and the purity of the chemicals used in this study. All chemicals were used without further purification.

Theory

The model used to describe the systems containing water-soluble organic hydrate formers is based on the equivalence of the chemical potentials in both the hydrate phase and the aqueous liquid phase.

Table 1. Suppliers and Purity of the Pure Substances Used

Substance	Suppliers	Purity in Mol %
Methane	Air Products	99.995
Tetrahydrofuran	J. T. Baker	> 99
1,3-Dioxolane	Merck-Schudchardt	> 99
Tetrahydropyran	Acros	> 99
Water		Distilled

In all the models proposed so far, the chemical potential is given as the difference between the chemical potential in the aqueous liquid or hydrate phase and the chemical potential in a theoretical empty hydrate lattice:

$$\mu_w^L = \mu_w^H \tag{1}$$

$$\Delta\mu_w^L = \mu_w^\beta - \mu_w^L = \Delta\mu_w^H = \mu_w^\beta - \mu_w^H. \tag{2}$$

Van der Waals and Platteeuw (1959) derived an expression for the chemical potential of water in the hydrate phase. Parrish and Prausnitz (1972) introduced modifications to include the description of mixed hydrates:

$$\Delta\mu_w^H = -R_C \cdot T \cdot \sum_i \nu_i \cdot \ln\left(1 - \sum_k \theta_{ki}\right). \tag{3}$$

The fractional occupancy of the hydrate cavity i by guest molecule type k can be expressed by using the following equation:

$$\theta_{ki} = \frac{C_{ki} \cdot f_k}{1 + \sum_j C_{ji} \cdot f_j}. \tag{4}$$

The description of the fractional occupancy is very similar to the equation describing Langmuir adsorption isotherms. The C_{ki} in the equation is therefore called the Langmuir constant.

The fugacities of the hydrate formers like methane can be calculated from an equation of state. For all hydrate formers in a hydrocarbon phase, an equation of state like the Peng-Robinson or Soave-Redlich-Kwong equations of state can be used. Due to the low fugacities of the water–soluble hydrate formers in the systems investigated (acetone, 1,3-dioxolane, and THF), it is assumed that the vapor phase consists of pure methane. The Soave-Redlich-Kwong equation of state (Soave, 1972) has been used to calculate this fugacity.

The fugacity of the water-soluble hydrate formers in the systems studied has been calculated from the aqueous liquid phase by using the composition of the aqueous liquid phase and the activity coefficient of the soluble hydrate former:

$$f_k = x_k \cdot \gamma_k \cdot \Phi_k^{\text{sat}} \cdot P_k^{\text{sat}} \cdot e^{\frac{V_k^L \cdot (P - P^{\text{sat}})}{R_C \cdot T}}. \tag{5}$$

The vapor pressures can be calculated using the Antoine equation. The Antoine constant for acetone and THF are given by Reid et al. (1987), and for 1,3-dioxolane in the Chemistry Data Series (Gmehling et al., 1981). The activity coefficients are calculated from the Van Laar equation in the case of acetone and THF, and from the Wilson equation in the case of 1,3-dioxolane. The constants in the Van Laar equation are calculated from data on the activity coefficients at infinite dilution. The activity coefficients at infinite dilution are given by Kojima et al. (1997) and in the Chemistry Data Series (Gmehling et al., 1994a). Matching the data to the equation given below was successful:

$$\ln(\gamma_k^\infty) = \frac{\alpha}{T} + \beta. \tag{6}$$

The activity coefficients for 1,3-dioxolane are calculated from the Wilson constants given by Francesconi et al. (1980) based on vapor–liquid equilibria. In every investigated system extrapolations had to be made to use the literature data in the experimental temperature range.

The Langmuir constants for the fractional occupancy can be calculated from the following summation of all water–guest-molecule interactions inside the hydrate cage:

$$C_{ki} = \frac{4\pi}{k \cdot T} \cdot \int_0^R e^{-(\omega(r))/(k \cdot T)} \cdot r^2 \, dr. \tag{7}$$

The spherical symmetrical cell potential $\omega(r)$ is calculated using the Kihara approach for the interaction between the guest molecule and the surrounding water molecules. The expression for the Kihara potential, as given by McKoy and Sinanoglu (1963), has been used to calculate $\omega(r)$:

$$\omega(r) = 2 \cdot z \cdot \epsilon \cdot \left[\frac{\sigma^{12}}{R^{11} r} \cdot \left(\delta^{10} + \frac{a}{R} \cdot \delta^{11}\right) - \frac{\sigma^6}{R^5 r} \cdot \left(\delta^4 + \frac{a}{R}\delta^5\right)\right], \tag{8}$$

with

$$\delta^N = \frac{1}{N} \cdot \left[\left(1 - \frac{r}{R} - \frac{a}{R}\right)^{-N} - \left(1 + \frac{r}{R} - \frac{a}{R}\right)^{-N}\right]. \tag{9}$$

The constants used in the description for the hydrate phase (radius of hydrate cage R, coordination number z, number of cages per water molecule ν) are given by Sloan (1998) and Jager et al. (1999). The Kihara parameters are known for methane and are also given by Sloan (1998) and Jager et al. (1999). The Kihara parameters for acetone, 1,3-dioxolane, and THF are calculated in this study by fitting the model to the experimental data.

The chemical potential of water in the aqueous liquid phase can be calculated from an equation given by Holder et al. (1980):

$$\frac{\Delta\mu_w^L}{R_C \cdot T} = \frac{\Delta\mu_w^0}{R_C \cdot T_0} - \int_{T_0}^T \frac{\Delta H_w^L}{R_C \cdot T^2} dT + \int_0^p \frac{\Delta V_w^L}{R_C \cdot T} dp - \ln(\gamma_w \cdot x_w). \tag{10}$$

Values for $\Delta\mu_w^0$ and ΔV_w^L, and a relation to describe the reference enthalpy, can be found in Sloan (1998) and Jager et al. (1999).

Table 2. Experimental and Modeling Results $H - L_w - V \rightarrow L_w - V$ Transition Water–Methane–THF System

T (K)	p (MPa)	T (K)	p (MPa)	T (K)	p (MPa)
$X = 0.0107$		$X = 0.0500$		$X = 0.1008$	
289.54	2.051	293.11	2.051	292.77	2.051
293.02	3.550	296.76	3.549	296.73	3.549
295.66	5.049	299.28	5.049	299.07	5.049
297.48	6.549	301.05	6.548	300.97	6.548
299.07	8.048	302.50	8.047	302.31	8.048
300.32	9.548	303.74	9.547	303.52	9.547
301.17	11.047	304.73	11.047	304.56	11.047
301.81	12.047	305.52	12.547	305.45	12.547
302.18	12.547	306.22	14.046	306.23	14.047
303.01	14.047				

Note: x = mol % THF relative to water.

The activity coefficients are again calculated from the Van Laar equations and the Wilson equations. The same considerations as those made for the activity coefficients of the soluble hydrate formers apply here. Activity coefficient data have been taken from various literature sources (Koijma et al., 1997; Francesconi et al., 1980; Gmehling et al., 1994b).

There are two additional assumptions regarding hydrate structure and methane solubility that should be made. The first assumption is that the water–methane–water-soluble organic compound systems form structure II hydrates. This statement is supported by the findings presented in several publications (Jager et al., 1999; Saito et al., 1996; Sum et al., 1997; Subramanian and Sloan, 1999; Saito, personal communication, 1996). Another assumption is that the solubility of methane in the aqueous liquid phase is very small. This means that the activity coefficients can be calculated from literature data for activity coefficients at infinite dilution in the binary water–water-soluble hydrocarbon without methane systems. However, in determining the composition of the aqueous liquid phase, as used in the model. the concentrations of all the components, including methane, are considered. Methane solubility is calculated by means of the Krichevsky-Kasarnovsky equation (Krichevsky and Kasarnovsky, 1935).

The compositions of both the aqueous liquid phase and the vapor phase are not influenced by the composition of the hydrate phase, because the calculations determine the conditions under which the last hydrate crystal disappears. This means that an infinitely small amount of hydrate is present that is far too small to influence the composition of the other two phases. Based on these assumptions, the composition of the aqueous phase at the hydrate dissolution conditions is equal to the composition that was inserted into the Cailletet tube.

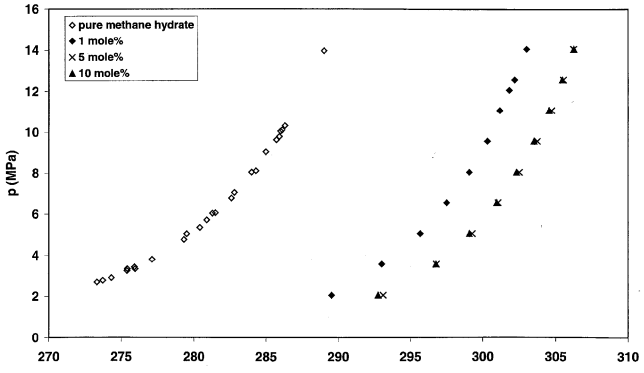

Figure 1. p,T-Diagram of the H-L_w-$V \rightarrow L_w$-V transitions in the water–methane–THF system.

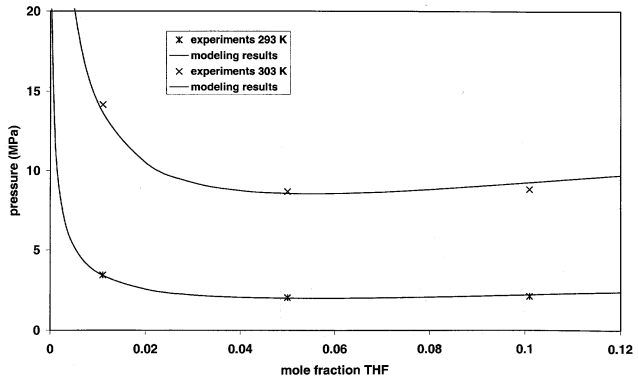

(a)

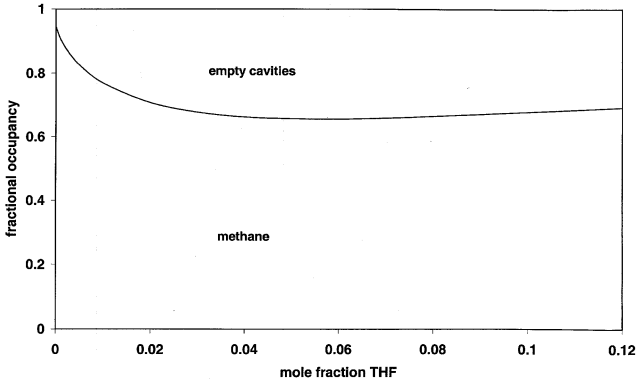

(b)

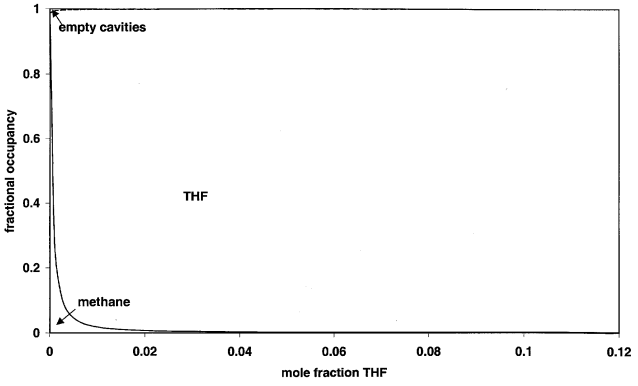

(c)

Figure 2. (a) p,x-Diagram of the H-L_w-$V \rightarrow L_w$-V transitions in the water–methane–THF system; (b) cumulative fractional occupancy of the 5^{12} cavities at 293 K; (c) cumulative fractional occupancy of the $5^{12}6^4$ cavities at 293 K.

The model developed to describe the hydrate formation of systems containing water-soluble organic hydrate formers consists of two parts. The first regression part calculates Kihara parameters out of a set of experimental data points, while the second prediction part calculates the $H - L_w - V \rightarrow L_w - V$ transition pressure given the temperature and composition. The second part requires the Kihara parameters calculated in the first part.

Two Kihara parameters, ϵ and σ, are fitted to the experimental data. Parameter a is calculated using the method proposed by Tee et al. (1966). The critical pressure and temperature and the acentric factor, which are necessary in the calculation, have been taken from Reid et al. (1987). In the case of 1,3-dioxolane, these data were not available, so the Ambrose method as described by Reid et al. (1987) is used to obtain the critical data. The Kihara parameters are calculated for each data point. It emerged that parameter ϵ is the most important parameter to fit the model to the experimental data.

Results and Discussion

Experimental results

Table 2 displays the experimental data on $H - L_w - V \rightarrow L_w - V$ transition in the water–methane–THF system. These data are graphically shown as isopleths in the pressure vs. temperature plot in Figure 1. Two isotherms have been calculated, based on the experimental data. The isotherms were obtained by fitting an exponential equation to the experimental data of each isopleth. This approach gave a very good correlation, which is suitable to use for interpolation. Figure 2a shows the isotherms in a pressure vs. composition diagram. The data for pure methane hydrate as used in Figure 2a are taken from the literature (De Roo et al., 1988; Deaton and Frost, 1946; McLeod and Campbell, 1961).

The data on the $H - L_w - V \rightarrow L_w - V$ transition in the water–methane–1,3-dioxolane system are reported in Table 3. The isopleths are plotted in the pressure vs. temperature plot in Figure 3. In this system, the same procedure as mentioned previously is used to transform isopleths into isotherms. The results are shown in Figure 4.

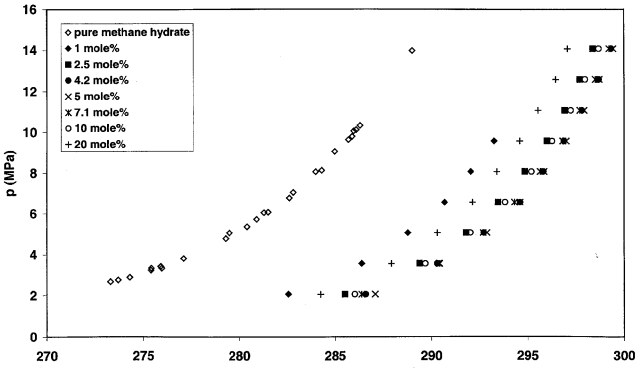

Figure 3. *p,T*-Diagram of the H-L_w-$V \rightarrow L_w$-V transitions in the water–methane–1,3-dioxolane system.

For the water–methane–THP system, only one composition has been measured, due to the limited solubility of THP in water. The experimental data are shown in Table 4. Because only one composition has been measured, it is not possible to construct isotherms.

Modeling results

The calculated Kihara parameters are shown in Table 5. The parameters have been fitted to experimental hydrate data, and therefore represent the gas–water interaction.

The model just discussed has been applied to the experimental results for the water–methane–THF and water–methane–1,3-dioxolane systems, as well as to the wa-

Table 3. Experimental and Modeling Results $H - L_w - V \rightarrow L_w - V$ Transition Water–Methane–1,3-Dioxolane System

T (K)	p (MPa)	T (K)	p (MPa)	T (K)	p (MPa)	T (K)	p (MPa)
$X = 0.0099$		$X = 0.0250$		$X = 0.0420$		$X = 0.0499$	
282.55	2.061	285.53	2.059	286.60	2.056	287.10	2.061
286.38	3.556	289.39	3.555	290.30	3.554	290.40	3.555
288.77	5.054	291.82	5.054	292.74	5.053	292.91	5.054
290.69	6.553	293.49	6.553	294.61	6.552	294.60	6.552
292.06	8.052	294.86	8.051	295.81	8.051	295.84	8.051
293.27	9.551	295.99	9.551	296.88	9.551	297.00	9.551
		296.92	11.051	297.83	11.051	297.94	11.050
		297.70	12.551	298.70	12.551	298.72	12.550
		298.39	14.050	299.35	14.050	299.44	14.050
T (K)	p (MPa)	T (K)	p (MPa)	T (K)	p (MPa)	T (K)	p (MPa)
$X = 0.0708$		$X = 0.1002$		$X = 0.2002$			
286.38	2.057	286.03	2.055	284.24	2.053		
290.43	3.553	289.03	3.553	287.93	3.551		
292.71	5.053	292.04	5.051	290.31	5.051		
294.33	6.552	293.85	6.551	292.16	6.551		
295.65	8.051	295.20	8.050	293.42	8.050		
296.83	9.551	296.26	9.550	294.60	9.549		
297.70	11.051	297.23	11.049	295.54	11.049		
298.52	12.550	297.98	12.549	296.45	12.549		
299.23	14.050	298.69	14.049	297.07	14.048		

Note: x = mol % 1,3-dioxolane relative to water.

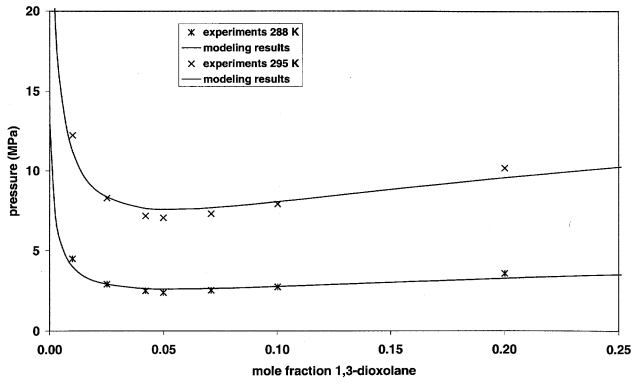

(a)

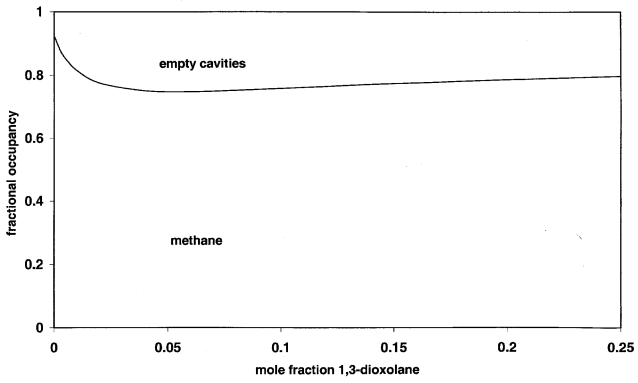

(b)

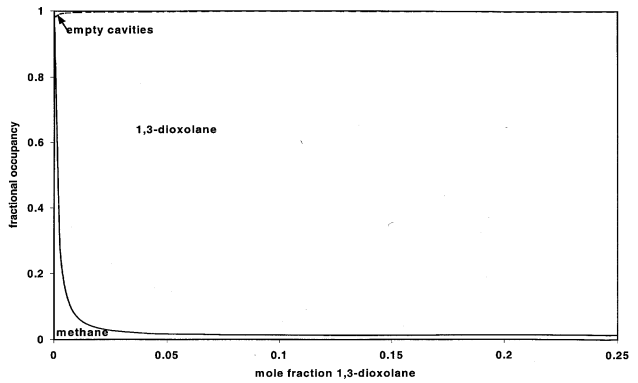

(c)

Figure 4. (a) p,x-Diagram of the H-L_w-$V \rightarrow L_w$-V transitions in the water–methane–1,3-dioxolane system; (b) cumulative fractional occupancy of the 5^{12} cavities at 288 K; (c) cumulative fractional occupancy of the $5^{12}6^4$ cavities at 288 K.

ter–methane–acetone system, as reported by Mainusch et al. (1997) and Ng and Robinson (1996).

The error percentage has been calculated as:

$$\text{Error}\,\% = \frac{(p_{\text{calc}} - p_{\text{exp}})}{p_{\text{exp}}} \cdot 100\%. \qquad (11)$$

Table 4. Experimental Results of the Phase-Transition $H - L_w - V \rightarrow L_w - V$ in the Water–Methane–THP system

T (K)	P (MPa)	T (K)	P (MPa)
$X = 0.0098$		$X = 0098$	
2.051	288.31	9.547	299.87
3.550	292.46	11.047	300.82
5.049	295.10	12.547	301.85
6.548	297.07	14.047	302.58
8.048	298.76		

Note: x = mol fraction THP relative to water.

The average absolute deviations (AADP%) are calculated by means of the equation:

$$\text{AADP}\,\% = \frac{|\text{error}\,\%|}{N_{\text{exp}}}. \qquad (12)$$

Table 6 presents an example of the calculation results for one of the three compositions of the water–methane–THF system and a comparison with the experimental data points. Figure 5a represents the calculation of the hydrate disappearance conditions, the $H - L_w - V \rightarrow L_w - V$ transition in a pressure vs. temperature plot. The example shows a composition of 5 mol % THF relative to water. Figure 2a displays the pressure vs. composition diagram of the water–methane–THF system. The correspondence between the experimental results and the calculation is excellent, as can be seen from both the tables and the figures.

Figure 4a shows the pressure vs. composition plot of the water–methane–1,3-dioxolane system. The differences between the experimental and the modeling results are somewhat larger than in the water–methane–THF system, but the description is still accurate.

Figure 6a presents an example of a pressure vs. temperature plot of the water–methane–acetone system. Figure 7a gives the plot of the pressure vs. composition diagram. As can be seen from Figure 6a, the $H - L_w - V \rightarrow L_w - V$ transition of the water–methane–acetone system is modeled very accurately. With concentrations of acetone that are higher than 20 mol %, however, the model does not correspond very well with the experimental data. The p,x-plot in Figure 7a shows this graphically. The calculations between 9 and 20 mol % acetone relative to water show a considerable AADP%, but Figure 7a shows a rather large scatter in the experimental data in the concentration range. The model prediction based on the experimental results of both literature sources is quite accurate. The calculation relation lies in the middle of the mass of experimental data coming from both sources. At high acetone concentrations, the deviation between exper-

Table 5. Calculated Kihara Parameters for the Applied Water-Soluble Organic Compounds (Organic Compound–Water Interaction)

	a in Å	σ in Å	ϵ/k in K
Acetone	1.024	3.3	224.2
1,3-Dioxolane	0.927	3.3	236.2
THF	0.881	3.6	296.4

Table 6. Experimental and Modeling Results $H - L_w - V \rightarrow L_w - V$ Transitions in the Water–Methane–THF System

				Fractional Occupancies			
				Small Cavities		Large Cavities	
T (K)	p (MPa)	P_{calc} (MPa)	Error %	Methane	THF	Methane	THF
293.11	2.051	2.030	−1.02	0.659	0.000	0.003	0.997
296.76	3.549	3.530	−0.54	0.744	0.000	0.004	0.995
299.28	5.049	5.077	0.55	0.789	0.000	0.006	0.994
301.05	6.548	6.521	−0.41	0.817	0.000	0.007	0.993
302.50	8.047	7.991	−0.70	0.836	0.000	0.008	0.992
303.74	9.547	9.500	−0.49	0.851	0.000	0.009	0.991
304.73	11.047	10.903	−1.30	0.863	0.000	0.009	0.990
305.52	12.547	12.164	−3.05	0.871	0.000	0.010	0.990
306.22	14.046	13.398	−4.61	0.878	0.000	0.010	0.989
AADP% 1.409							

Note: 5 mol % THF relative to water.

imental data and modeling results becomes quite large. This phenomenon was also observed by Jager et al. (1999) modeling the water–methane–1,4-dioxane system.

A detailed set of modeling results for all the mentioned compositions of the system containing THF, 1,3-dioxolane, and acetone as the organic compound is available on the Internet: http://www.dct.tudelft.nl/ic/hydrates.htm.

Discussion of the experimental results

Figure 8 contains the isotherms of the three systems measured in this study, the data for the water–methane–acetone system by Ng and Robinson (1996) and Mainusch et al. (1997), and the water–methane–1,4-dioxane data by Jager et al. (1999). The survey shows that the pressure-reducing effect is dependent on the applied organic compound. Another observation is the dependence of the pressure-reduction effect on the structure of organic molecules. The cyclic ethers considered in this study and in the study by Jager et al. show a certain analogy. THF and 1,3-dioxolane are five-membered cyclic compounds, while THF and 1,4-dioxane are six-membered cyclic compounds. THF and THP have one oxygen atom in the ring, and 1,3-dioxolane and 1,4-dioxane contain two oxygen atoms. Looking at Figure 8, it can be seen that mixed hydrates of five-membered cyclic ethers have a lower equilibrium pressure than the mixed hydrates of six-membered cyclic ethers when comparing the hydrates with the same number of oxygen atoms in the ring of the cyclic ether. Furthermore, mixed hydrates of cyclic ethers with one oxygen atom have lower equilibrium pressures than mixed hydrates of cyclic ethers with two oxygen atoms. These facts suggest that the five-membered cyclic compound without any oxygen atoms, cyclopentane, would even have a lower equilibrium pressure, as confirmed by Tohidi et al. (1997a,b). The systematic differences can be explained by differences in size and polarity of the molecules. Apparently, five-membered cyclic compounds fit better in the cavities of the hydrate than six-membered cyclic compounds. Very polar compounds are very good hydrate inhibitors. The smaller polarity of cyclic compounds with fewer oxygen atoms in the ring of the molecule causes less distortion of the hydrate lattice and apparently leads to more stable mixed hydrates.

The pressure-reducing effect of the organic compounds can be calculated as the ratio of the equilibrium pressure of the mixed hydrate and the equilibrium pressure of pure methane hydrate. The suppression varies between about 50% of the equilibrium pressure of methane hydrate for acetone–methane mixed-hydrate systems to about 92% for THF–methane mixed hydrate at 290 K and 5 mol % organic compound relative to water. The pressure-reducing ratio is slightly dependent on temperature. In Figure 9 the dependency of the pressure suppression ratio vs. mole fraction 1,3-dioxolane relative to water is plotted for three different isotherms.

Figure 8 clearly shows that the pressure minimum is found at about the same concentration of organic compounds in every system displayed. Because the correlation in the pressure vs. mole fraction organic compound is rather flat around the pressure minimum, it is very difficult to determine the exact minimum with great accuracy. The minimum is between 5 and 6 mol % relative to water for each of the systems compared in Figure 8.

The position of the pressure minimum (5–6 mol % relative to water) corresponds to the ratio between the number of large cavities and water molecules in a structure II hydrate unit cell (1/17 or 5.88 mol % relative to water). Based on this determination, we assume that the water–methane–applied organic compound systems form structure II mixed hydrates. Saito et al. (1996) and Saito (personal communication, 1996) support this assumption. Sloan and coworkers (Sum et al., 1997; Subramanian and Sloan, 1999) also use this assumption in their investigations of cavity occupation, hydration numbers, and formation kinetics with Raman spectroscopy.

Discussion of the modeling results

The modeling results are, in general, very accurate. For concentrations up to 20 mol % organic compound relative to water, the differences between experimental data and modeling results are quite small.

At very low concentrations (1 mol %) the deviations are larger than at somewhat higher concentrations. A possible explanation for this is the strong dependence on the organic concentration, as can be seen in Figures 2a, 4a, and 7a. A small error in the concentration of the organic compound can cause large errors. Another error can be caused by the distribution of the organic compound over the aqueous liquid phase and the vapor phase. We assume the amount of organic compound in the vapor to be zero. If this assumption is not valid,

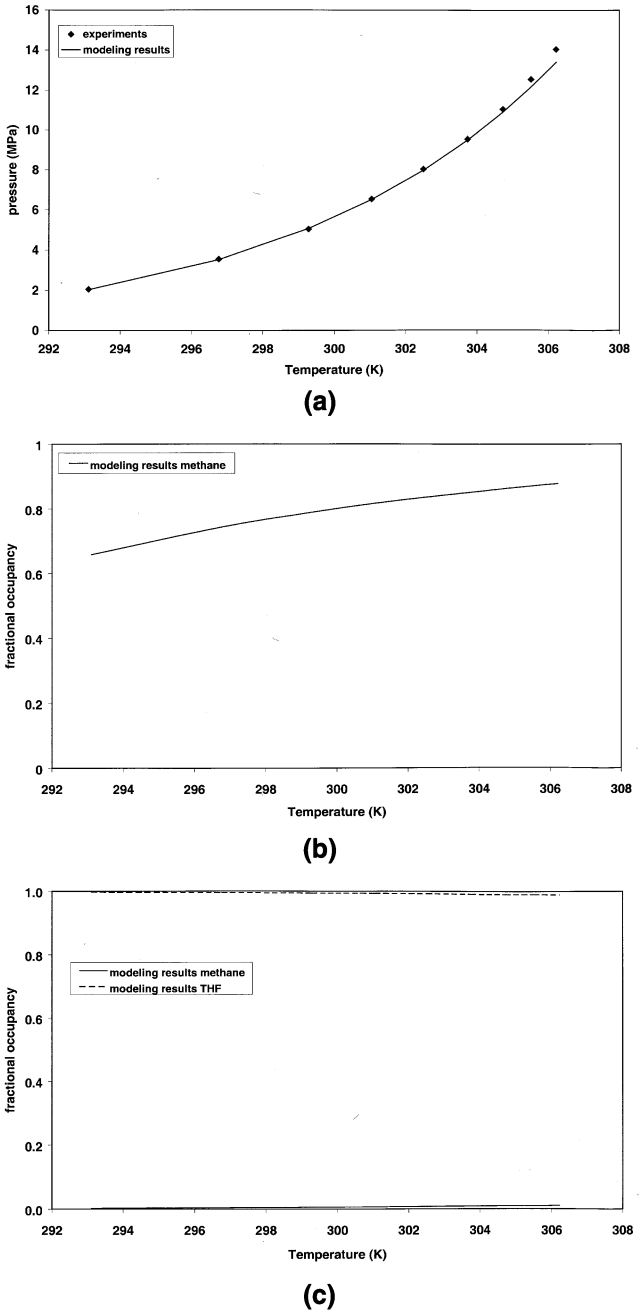

Figure 5. (a) p,T-Diagram of the $H\text{-}L_w\text{-}V \rightarrow L_w\text{-}V$ transitions in the water–methane–THF system (5 mol % THF relative to water); (b) methane fractional occupancy in 5^{12} cavities [same composition as in (a)]; (c) methane and THF fractional occupancy $5^{12}6^4$ in cavities [same composition as in (a)].

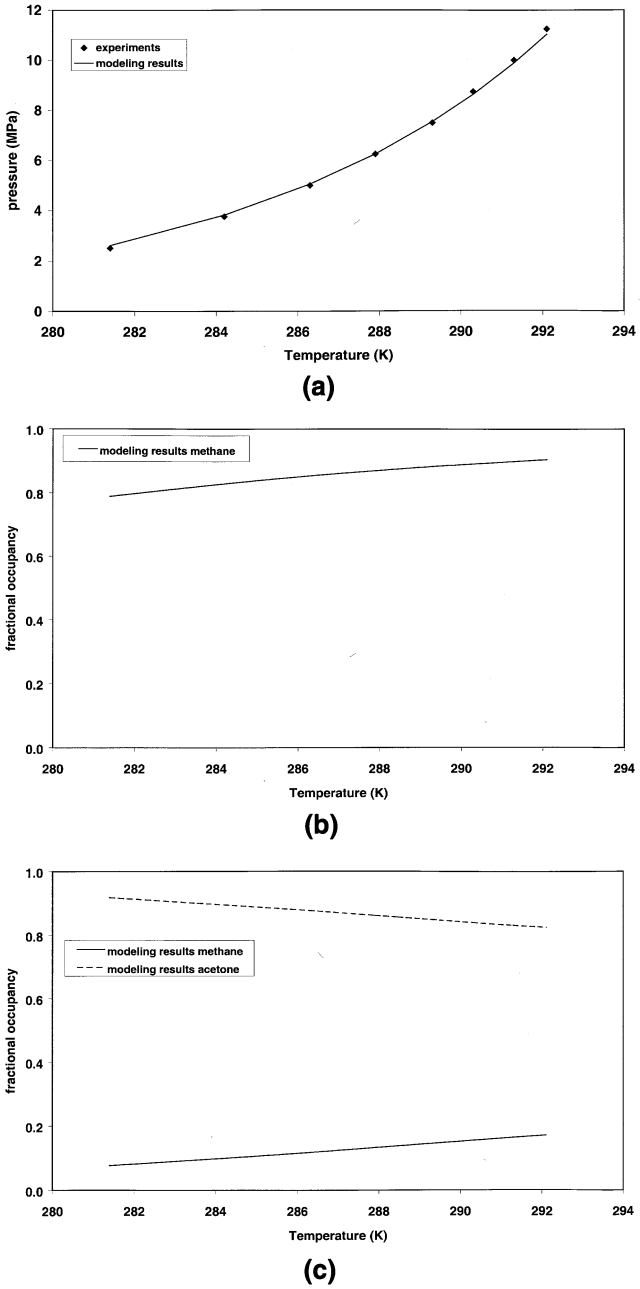

Figure 6. p,T-Diagram of the $H\text{-}L_w\text{-}V \rightarrow L_w\text{-}V$ transitions in the water–methane–acetone system (3.33 mol % acetone relative to water) (*Data*: Mainusch et al. (1997)]; (b) methane fractional occupancy in 5^{12} cavities [same composition as in (a)]; (c) methane and acetone fractional occupancy in $5^{12}6^4$ cavities [same composition as in (a)].

this has the largest impact on the calculations with low concentrations of water-soluble hydrate formers.

At very large concentrations, the deviation between the model and the experimental data becomes substantial. We assumed that the methane solubility in the aqueous liquid phase would be very limited. That assumption enabled us to treat the aqueous liquid phase as a binary liquid that could be described according to binary activity coefficient data. The high concentrations of organic compound in the liquid phase will increase the methane solubility, and this will influence the water and the water-soluble hydrate-former concentration in the liquid phase. Moreover, this brings in doubt the

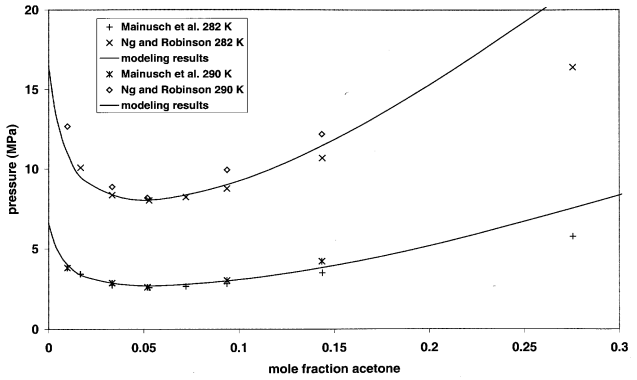

(a)

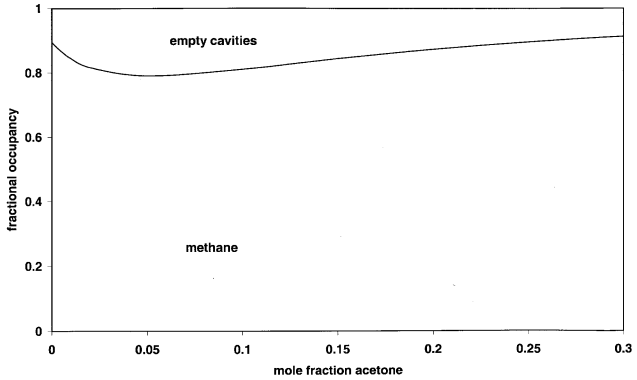

(b)

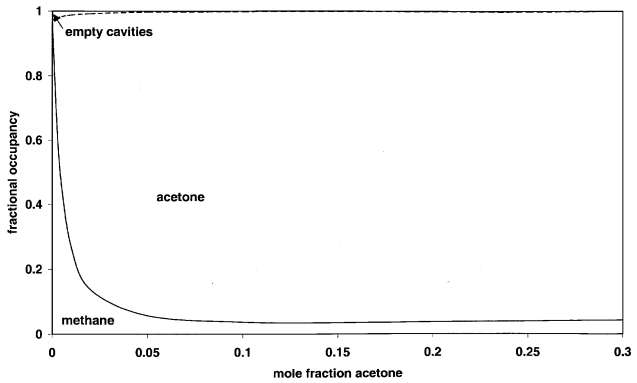

(c)

Figure 7. (a) p,x-Diagram of the H-L_w-$V \rightarrow L_w$-V transitions in the water–methane–acetone system; (b) cumulative fractional occupancy of the 5^{12} cavities at 282 K; (c) cumulative fractional occupancy of the $5^{12}6^4$ cavities at 282 K.

validity of the assumption that the activity coefficients can be taken from binary data. Ternary data for these systems are not available in the literature, as far as we know.

The pressure minimum, as observed in own and the experimental results in the literature, is also found in the modeling results. In an earlier publication (Jager et al., 1999) and in the previous section, we also considered the position of the pressure minimum and concluded that the position of the

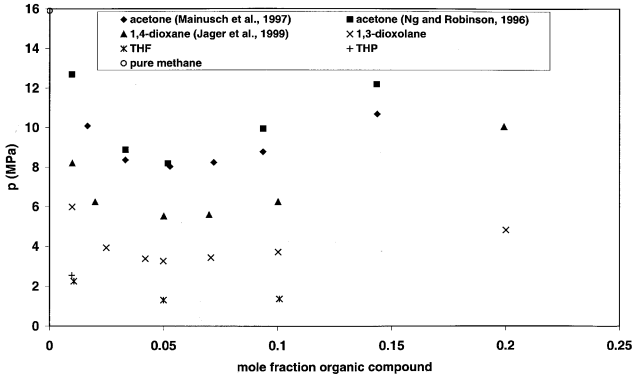

Figure 8. Survey p,x-diagram of the H-L_w-$V \rightarrow L_w$-V transitions in the water–methane–organic compound system at $T = 290$ K.

minimum is closely related to the ratio of large cavities to water molecules in structure II hydrates. We interpreted this as a strong indication that the hydrates formed were indeed structure II hydrates. We regard the present modeling research as further evidence for this statement. The model has been used to analyze the position of the pressure minimum when water-soluble organic compounds are added. Table 7 shows the position and pressure of the pressure minimum of the isotherms displayed in Figures 2, 4, and 7. It is clear that the position of the pressure minimum is only slightly dependent on the temperature and on the applied additive. The same observation has been reported by Jager et al. (1999) for the water–methane–1,4-dioxane system. The deviation from the ratio between the number of large cavities and the number of water molecules in structure II hydrate (0.0588) and the modeling results is small.

Consideration of the fractional occupancies of the hydrate cavities

Besides calculation of the hydrate disappearnce conditions, we used the model to calculate the composition of the hydrate phase. Although we lack the experimental data to validation our results, we are quite confident that the calculated

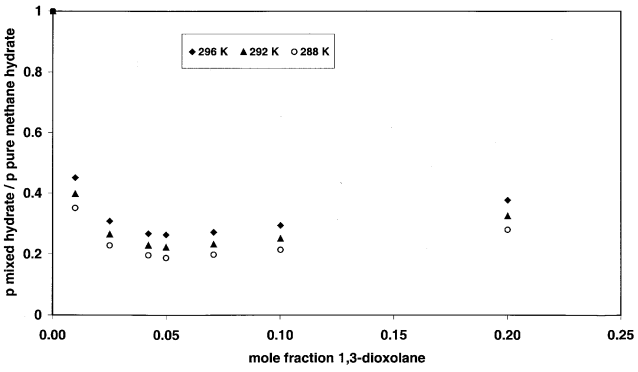

Figure 9. Survey pressure ratio vs. x-diagram of the H-L_w-$V \rightarrow L_w$-V transitions in the water–methane–1,3-dioxolane system.

Table 7. Modeling of the Position of the Pressure Minimum in Selected Isotherms

Isotherm (K)	Position Pres. Min. (Mol Fract. Organic Compound)	Pres. (MPa)	Fractional Occupancies			
			Small Cavities		Large Cavities	
			Methane	Organic Compound	Methane	Organic Compound
1,3-Dioxolane						
288	0.0547	2.614	0.747	0.016	0.000	0.982
295	0.0547	7.608	0.861	0.038	0.000	0.961
THF						
293	0.0554	1.989	0.656	0.003	0.000	0.997
303	0.0550	8.551	0.842	0.008	0.000	0.992
Acetone						
282	0.0525	2.700	0.791	0.054	0.000	0.942
290	0.0494	8.040	0.885	0.112	0.000	0.885

fractional occupancies of the hydrate cavities represent the physical behavior. This composition is obtained in the calculation route toward the hydrate equilibrium pressure of the hydrate system. Because the calculated hydrate equilibrium pressures and the experimental data show good correspondence, we believe that the cavity fillings that the model provides also have physical significance.

The model has been used to calculate the hydrate composition between 0 mol % water-soluble organic hydrate former and the highest experimental concentration. If no water-soluble hydrate former is present, the system will form single-hydrate methane with structure I instead of structure II. The figures show a structure II calculation at 0 mol % water-soluble hydrate former, but it must be clear that this calculation has only a theoretical meaning and will not be reached in practice.

In Figures 6b and 6c, the calculated fractional occupancies of methane–acetone mixed hydrate are shown. In Figure 6, the concentration of acetone in the system is 3.33 mol % relative to water. Figure 6b shows the calculated methane occupancy in the small 5^{12} cavities. Because acetone is too large to fit in these small cavities, the rest of the cavities is empty. Figure 6c shows the occupancies in the large $5^{12}6^4$ cavities. The fraction of empty large cavities is small.

The calculated results correspond with the hydrate disappearance conditions as shown in Figure 6a. In Figures 6b and 6c, it can be seen that the fractional occupancy of methane increases with higher temperatures. The increasing fractional occupancy, as depicted in Figures 6b and 6c, is coupled with not only higher temperatures, but also with higher pressures. In Figure 6c it appears that the fractional occupancy of acetone in the large hydrate cavities decreases with higher temperatures and pressures. This observation can be interpreted as a shift in the competitive adsorption equilibrium. The results are an illustration of the Langmuir adsorption analogy in the Van der Waals and Platteeuw hydrate equilibrium theory.

Figures 5b and 5c contain the results of the same calculations for methane–THF hydrate with a THF concentration of 5 mol % relative to water. The results show the same trends, but the values of the occupancies differ significantly. The methane occupancy in the large $5^{12}6^4$ cavity is almost reduced to zero and the THF occupancy is almost 100%. The methane filling of the small cavities is also lower in the case of methane–THF hydrate.

Figures 2b, 2c, 4b, 4c, 7b, and 7c depict the fractional occupancies as a function of the mole fraction organic compound. The figures show that the methane filling of the large $5^{12}6^4$ cavities decreases rapidly when some organic compound is added to the system, while the fractional occupancy of the organic compound grows rapidly. The methane occupancy in the small 5^{12} cavities exhibits a minimum between 4.94 and 5.54 mol % organic compound, depending on the compound and temperature. This minimum coincides with the minimum in the pressure vs. composition plots in Figures 2b, 2c, 4b, 4c, 7b, and 7c. This observation complies with our earlier remarks and presumptions about the structure of the hydrates studied.

The results of the fractional occupancy calculation also show some other trends. Figures 6 and 7 show the effect of acetone on the methane occupancies in both the small and the large cavities as a function of both temperature and composition. Figures 2 and 5 show the same information for THF as organic compound. As discussed before, THF has the strongest hydrate equilibrium pressure reducing effect. Figures 2b, 2c, 5b, and 5c show the methane occupancies of the cavities. It is quite clear that the methane occupancy of both kinds of cavity is more affected in the system with THF than in the acetone system. The calculation for the system containing 1,3-dioxolane shows the same trend. This means that the organic compound with the best equilibrium pressure reducing capabilities also has the largest impact on the methane content of the hydrate phase. This observation has serious negative implications for the application of hydrates as a storage or transportation medium for natural or other gases.

Conclusions

The $H - L_w - V \rightarrow L_w - V$ hydrate disappearance conditions have been determined experimentally for three different water–methane–water-soluble organic compound systems. The examined organic compounds are 1,3-dioxolane, tetrahydrofuran (THF), and tetrahydropyran (THP). In addition to this experimental study, we also calculated the hydrate disappearance conditions, $H - L_w - V \rightarrow L_w - V$ transition, for various water–methane–water-soluble organic compound systems. In the modeling study, the organic compounds that were used were THF, 1,3-dioxolane, and acetone.

The measurements showed a sharp decrease in hydrate equilibrium pressures upon addition of small amounts of the water-soluble organic compounds. The maximum pressure-reducing effect was reached upon addition of around 5 to 6 mol % organic compound relative to water. The pressures are reduced down to 20% of the equilibrium pressure without the addition of an organic compound for the water–methane–1,3-dioxolane system and 8% for the water–methane–THF system.

The calculated results correspond well with experimental data. The experimentally observed pressure-reducing effect of adding small amounts of water-soluble organic compound can be modeled using the approach presented in this study. The average absolute deviation of the pressure (AADP) in the water–methane–THF system is between 2 and 4%. The deviations in the water–methane–1,3-dioxolane system are between 2 and 12%, while they are between 2 and 10% in the water–methane–acetone system. With high acetone concentrations (above 20 mol % relative to water), the deviations increase dramatically. The explanation for this is found in the limitations of the assumption on the solubility of methane in the aqueous liquid phase.

This contribution also considered the fractional occupancies of the hydrate cavities, as can be calculated with the same model. The results of the consideration show a very interesting insight in the phenomena that happen in mixed hydrate formation. The reduced hydrate equilibrium pressure can be attributed to the reduced methane content in both kinds of cavities and the partial replacement by the water-soluble organic compound. The Langmuir adsorption analogy in the Van der Waals and Platteeuw theory (1959) is illustrated elegantly.

The position of the pressure minimum that has been found in both the experimental and the modeling results around 5 and 6 mol % organic compound relative to water is independent of the applied organic compound and temperature. The composition of the minimum corresponds very well with the ratio of large cavities to water molecules in structure II hydrates. This observation provides strong evidence that the hydrates in this study are structure II hydrates. Without spectroscopic evidence, it is impossible to draw a final conclusion.

Acknowledgments

The authors thank E.J.M. Straver, W. Poot, L.J. Florusse, and Th. W. de Loos for their valuable technical assistance and/or advice during this study. We also acknowledge the role of C.J. Peters in suggesting this investigation.

Notation

A = Kihara parameter, spherical potential hard core radius, Å
B = heat capacity temperature dependency, J/mol·K^2
C = Langmuir constant, Pa^{-1}
ΔC_p^0 = reference-heat-capacity difference, J/mol·K
f = fugacity, Pa
ΔH = enthalpy difference, J/mol
ΔH^0 = reference enthalpy difference, J/mol
k = Boltzmann constant, J/K
N = exponent in Kihara expression
P = pressure, Pa
P^{sat} = saturated pressure, Pa
r = distance to hydrate cavity center, Å
R = radius of hydrate cavity, Å
R_c = universal gas constant, J/mol·K
T = temperature, K
T_0 = melting point of water (273.15 K)
V = molar volume, J/mol
ΔV = volume difference, m^3/mol
x = mole-fraction liquid phase
z = coordination number

Greek letters

α = constant
β = constant
γ = activity coefficient
δ = Kihara delta function
ϵ = Kihara parameter, maximum attractive potential, J
θ = fractional cavity occupancy
μ = chemical potential, J/mol·K
$\Delta\mu$ = chemical potential difference, J/mol·K
$\Delta\mu^0$ = reference chemical potential difference, J/mol·K
σ = Kihara parameter, zero potential energy distance, Å
ν = stoichiometric constant
Φ^{sat} = fugacity coefficient at saturation pressure
$\omega(r)$ = interaction potential function

Subscripts and superscripts

i = i type of cavity
j = j type of molecule
k = k type of molecule
w = water property
exp = experimental value
calc = calculated value
H = property of the hydrate phase
L = property of the liquid phase
β = property of a theoretically empty hydrate lattice
∞ = infinite dilution

Literature Cited

Bennet, G. M., and W. G. Philip, "The Influence of Structure on the Solubilities of Ethers. Part II. Some Cyclic Ethers," *J. Chem. Soc.*, 1937 (1928).

Coorens, H. G. A., C. J. Peters, and J. de Swaan Arons, "Phase Equilibria in Binary Mixtures of Propane and Tripalmitin," *Fluid Phase Equilib.*, **40**, 135 (1988).

Danesh, A., B. Tohidi, R. W. Burgass, and A. C. Todd, "Benzene Can Form Gas Hydrates," *Trans. Inst. Chem. Eng., Part A*, **71**, 457 (1993).

Danesh, A., B. Tohidi, R. W. Burgass, and A. C. Todd, "Hydrate Equilibrium Data of Methyl Cyclopentane with Methane or Nitrogen," *Trans. Inst. Chem. Eng. Part A*, **72**, 197 (1994).

Deaton, W. M., and E. M. Frost, "Gas Hydrates and Their Relation to the Operation of Natural Gas Pipe Lines," U.S. Bureau of Mines Monographs 8 (1946).

De Loos, Th. W., H. J. van der Kooi, W. Poot, and P. L. Ott, "Fluid Phase Equilibria in the System Ethylene + Vinyl Chloride," *Delft Prog. Rep.*, **8**, 200 (1983).

De Roo, J. L., C. J. Peters, R. N. Lichtenthaler, and G. A. M. Diepen, "Occurrence of Methane Hydrate in Saturated and Unsaturated Solutions of Sodium Chloride and Water in Dependence of Temperature and Pressure," *AIChE J.*, **29**, 651 (1983).

Francesoni, R., C. Castellari, A. Arcelli, and F. Comelli, "Vapor-Liquid Equilibria in Mixtures of 1,3 Dioxolane–Water," *Can. J. Chem. Eng.*, **58**, 113 (1980).

Gemhling, J., U. Onken, and W. Arlt, *Vapor-Liquid Equilibrium Data Collection Aqueous-Organic Systems*, Suppl. 1, Chemistry Data Series, Vol. I, Part 1a, Dechema, Frankfurt (1981).

Gmehling, J., J. Menke, and M. Schiller, *Activity Coefficients at Infinite Dilution $C_1 - C_9$*, Chemistry Data Series, Vol. IX, Part 3, Dechema, Frankfurt (1994a).

Gmehling, J., J. Menke, and M. Schiller, *Activity Coefficients at Infinite Dilution C_{10}-C_{36} with O_2S and H_2O*, Chemistry Data Series, Vol. IX, Part 4, Dechema, Frankfurt (1994b).

Holder, G. D., G. Corbin, and K. D. Papadopoulos, "Thermodynamic and Molecular Properties of Gas Hydrates from Mixtures Containing Methane, Argon, and Krypton," *Ind. Eng. Chem. Fundam.*, **19**, 282 (1980).

Jager, M. D., R. M. de Deugd, C. J. Peters, J. de Swaan Arons, and E. D. Sloan, "Experimental Determination and Modeling of Structure II Hydrates in Mixtures of Methane + Water + 1,4-Dioxane," *Fluid Phase Equilib.*, **165**, 209 (1999).

Kojima, K., S. Zhang, and T. Hiaki, "Measuring Methods of Infinite Dilution Activity Coefficients and a Database for Systems Including Water," *Fluid Phase Equilib.*, **131**, 145 (1997).

Krichevsky, I. R., and J. S. Kasarnovsky, "Thermodynamical Calculations of Solubilities of Nitrogen and Hydrogen in Water at High Pressures," *J. Amer. Chem. Soc.*, **57**, 2168 (1935).

Mainusch, S., C. J. Peters, J. de Swaan Arons, J. Javanmardi, and M. Moshfeghian, "Experimental Determination and Modeling of Methane Hydrates in Mixtures of Acetone and Water," *J. Chem. Eng. Data*, **42**, 948 (1997).

McKoy, V., and O. Sinanoglu, "Theory of Dissocation Pressures of Some Gas Hydrates," *J. Chem. Phys.*, **38**, 2946 (1963).

McLeod, H. O., and J. M. Campbell, "Natural Gas Hydrates at Pressures to 10,000 psia," *J. Pet. Technol.*, **13**, 590 (1961).

Ng, H.-J., and D. B. Robinson, "New Developments in the Measurement and Prediction of Hydrate Formation for Processing Needs," *Ann. N.Y. Acad. Sci.*, **715**, 450 (1996).

Parrish, W. R., and J. M. Prausnitz, "Dissociation Pressures of Gas Hydrates Formed by Gas Mixtures," *Ind. Eng. Chem. Process Des. Dev.*, **11**, 26 (1972).

Reid, R. C., J. M. Prausnitz, and B. E. Poling, *The Properties of Gases and Liquids*, 4th ed., McGraw-Hill, New York (1987).

Saito, Y., T. Kawasaki, T. Okui, T. Kondo, and R. Hiraoka, "Methane Storage in Hydrate Phase with Water Soluble Guests," *Proc. Int. Conf. on Natural Gas Hydrates*, Toulouse, France, p. 459 (1996).

Sloan, E. D., *Clathrate Hydrates of Natural Gases*, Dekker, New York (1998).

Soave, G., "Equilibrium Constants from a Modified Redlich-Kwong Equation of State," *Chem. Eng. Sci.*, **27**, 1197 (1972).

Subramanian, S., and E. D. Sloan, "Molecular Measurements of Methane Hydrate Formation," *Fluid Phase Equilib.*, **158–160**, 813 (1999).

Sum, A. K., R. C. Burruss, and E. D. Sloan, "Measurement of Clathrate Hydrates via Raman Spectroscopy," *J. Phys. Chem. B*, **101**, 7371 (1997).

Tee, L. S., S. Gotoh, and W. E. Stewart, "Molecular Parameters for Normal Fluids," *Ind. Eng. Chem. Fundam.*, **5**, 363 (1966).

Tohidi, B., A. Danesh, R. W. Burgass, and A. C. Todd, "Equilibrium Data and Thermodynamic Modelling of Cyclohexane Gas Hydrates," *Chem. Eng. Sci.*, **51**, 159 (1996).

Tohidi, B., A. Danesh, A. R. Tabatabaei, and A. C. Todd, "Vapor-Hydrate Equilibrium Ratio Charts for Heavy Hydrocarbon Compounds: 1. Structure II Hydrates: Benzene, Cyclopentane, Cyclohexane, and Neopentane," *Ind. Eng. Chem. Res.*, **36**, 2871 (1997a).

Tohidi, B., A. Danesh, A. C. Todd, R. W. Burgass, and K. K. Østergaard, "Equilibrium Data and Thermodynamical Modelling of Cyclopentane and Neopentane Hydrates," *Fluid Phase Equilib.*, **138**, 241 (1997b).

Van der Waals, J. H., and J. C. Platteeuw, "Clathrate Solutions," *Adv. Chem. Phys.*, **2**, 1 (1959).

Manuscript received July 30, 1999, and revision received July 24, 2000.